

Concentration-dependent deuterium diffusion in diamondlike carbon films

T. Ahlgren,* E. Vainonen, J. Likonen,[†] and J. Keinonen

Accelerator Laboratory, University of Helsinki, P.O. Box 43, FIN-00014 University of Helsinki, Finland

(Received 27 August 1997)

Diffusion of deuterium in diamondlike carbon films has been studied. The deuterium concentration profiles in D⁺-ion-implanted films were measured by secondary-ion-mass spectrometry. A model is proposed to describe the experimental depth profiles. In this model it was assumed that atomic D is the diffusing species, whereas D in clusters is immobile. The results show that the concentration of D clusters relative to the total D concentration increases when the total D concentration decreases, leading to a concentration-dependent diffusion. The diffusion coefficients obtained for atomic D resulted in an activation energy of 2.9 ± 0.1 eV. The solid solubility of D was observed to decrease with increasing temperature. [S0163-1829(98)05716-6]

I. INTRODUCTION

There has been a recent growing interest in the synthesis and study of diamondlike carbon (DLC) films. Semiconducting diamond doped with different impurities would find applications in temperature-resistant and high-performance electronic devices.^{1,2} Properties of these devices depend on the presence of hydrogen, which acts as a passivator.^{3,4}

In the next step fusion device ITER (International Thermonuclear Experimental Reactor), carbon fiber composites (CFC's) have been chosen as the divertor armor material. In the presence of plasma, redeposition of sputtered carbon particles, diamondlike carbon films, and carbon-based composite films will take place. The uptake and release of deuterium and tritium from those films will significantly effect the recycling of D and tritium fuel, as well as tritium retention in the fusion device. Therefore, an understanding of the processes which involve trapping and retention of hydrogen isotopes in those films is important.

This work continues our studies on the migration of hydrogen isotopes in DLC films.⁵ The aim is to understand the evolution of the depth profiles of implanted D in DLC films at different temperatures, and to develop an analytical model to quantify this. Experimentally, we observe a concentration-dependent diffusion of D in DLC. According to the model developed to analyze the depth profiles, a fraction of D is immobile in clusters, while the rest diffuses as atomic D. The diffusion coefficient of atomic D, the ratio of the atomic D concentration to the concentration of D clusters, and the solid solubility of D in DLC are obtained. To our knowledge, there are no experimental data in the literature either on concentration-dependent D diffusion in DLC films or on the solid solubility of D in DLC. By using ion implantation, the effect of the surface diffusion was avoided, and the longer annealing times, compared to rapid thermal annealing, ensure steady-state diffusion.

II. EXPERIMENT

The DLC films studied were made by the company DIARC-Technology Inc. using the arc discharge method. Characterization of the films and the deposition method has been described in detail elsewhere.⁵ The samples were im-

planted by 54-keV D₂⁺ ions to a dose of 1×10^{16} ions cm⁻² (i.e., 27 keV/D and 2×10^{16} D⁺ ions cm⁻²). The implantations were performed at room temperature in the 100-keV isotope separator of the laboratory.

Annealing was done in a quartz-tube furnace (pressure below 0.05 mPa) at temperatures between 800 and 1100 °C. The annealing time varied from 30 min to 6 h.

The depth profiling of D atoms was carried out by secondary-ion-mass spectrometry (SIMS) at the Technical Research Center of Finland. The measurements were done with a double focusing magnetic sector SIMS (VG Ionex IX70S). The current of 5-keV O₂⁺ primary ions was typically 400 nA during depth profiling and the ion beam was raster scanned over an area of $240 \times 430 \mu\text{m}^2$. Crater wall effects were avoided by using a 10% electronic gate and 1-mm optical gate. The pressure inside the analysis chamber was 5×10^{-8} Pa during the analysis. The depth of the craters was measured by a profilometer (Dektak 3030ST). The uncertainty of the crater depth was estimated to be 5%. The D concentration of the as-implanted deuterium profile was normalized to the implanted dose.

III. DIFFUSION AND PAIRING MODELS

The diffusion model used in the current work assumes that hydrogen isotopes form immobile clusters and that the remaining atomic D is the diffusing species. To quantify this, we assume that the concentration of D clusters (C_{D_n}) containing n atoms is a function of the total D concentration (C_t)

$$C_{D_n} = K_n (C_t + F_n)^{B_n}, \quad n = 2, 3, \dots, N, \quad (1)$$

where n is the number of D atoms in a cluster, K_n is the clustering constant, B_n is the clustering exponent, and F_n is a constant to keep the concentrations of D clusters and of atomic D positive. The total D concentration can be written as

$$C_t = C_D + \sum_{n=2}^N n C_{D_n}, \quad (2)$$

where C_D is the concentration of single D atoms. The general concentration dependent diffusion equation is

$$\frac{\partial C_t}{\partial t} = \frac{\partial}{\partial x} \left(D_t^{\text{eff}}(C_t) \frac{\partial C_t}{\partial x} \right), \quad (3)$$

where $D_t^{\text{eff}}(C_t)$ is the effective diffusion coefficient at total concentration C_t . The flux equation is

$$D_t^{\text{eff}} \frac{\partial C_t}{\partial x} = D_a \frac{\partial C_D}{\partial x}, \quad (4)$$

where D_a is the diffusion coefficient for atomic D. The effective diffusion coefficient may be obtained from Eqs. (1), (2), and (4)

$$D_t^{\text{eff}} = D_a \left(1 - \sum_{n=2}^N n K_n B_n (C_t + F_n)^{B_n - 1} \right). \quad (5)$$

There are several works on hydrogen diffusion in silicon which propose diffusion of atomic hydrogen and formation of H_2 complexes.^{6,7} Recently Mehandru, Anderson, and Angus⁸ studied binding and diffusion of hydrogen in diamond. Investigations were done using the semiempirical atom superposition and electron delocalization molecular-orbital theory. It was concluded that H at a bond-centered (BC) site is more stable than at the tetrahedral and hexagonal interstitial sites. The pathway for H migration involving the motion from the BC site to a similar neighboring site using the high-density (110) planes is the most preferable. The calculated barrier for this case is 1.9 eV. Also calculated was the binding of a second H atom in the diamond lattice near the one already present at the BC site. The most stable site for the second hydrogen is the antibonding (AB) site forming a BC-AB hydrogen pair.

Taking into account the similarity of Si and diamond crystalline structures and the calculations of Ref. 8, we assume that the immobile clusters are deuterium pairs. Then Eqs. (1), (2) and (5) can be rewritten as

$$C_{D_2} = K(C_t + F)^B, \quad (6)$$

$$C_t = C_D + 2C_{D_2}, \quad (7)$$

$$D_t^{\text{eff}} = D_a [1 - 2KB(C_t + F)^{B-1}], \quad (8)$$

where C_{D_2} is the concentration of D pairs, K is the pairing constant, B is the pairing exponent, and F is a constant to keep the concentrations of D pairs and atomic D positive. All the diffusion parameters, diffusion coefficient D_a , pairing constant K , pairing exponents B and F , and solubility C_0 were obtained by least-squares fitting solving Eq. (3) numerically. Some calculations including the contribution of the mobile D pairs in the flux Eq. (4) were also made. No functional dependences for the fitting parameters K , B , and F were, however, observed in that case. Note that the assumption that the clusters are D pairs does not effect the results for diffusion of D atoms, it only approximates the immobile part of D.

Figure 1 presents the effective diffusion coefficient D_t^{eff} as a function of the total D concentration C_t for 900, 1000, and 1100 °C annealings. It can be observed that, at higher annealing temperatures, D_t^{eff} depends more strongly on the D concentration than at lower temperatures.

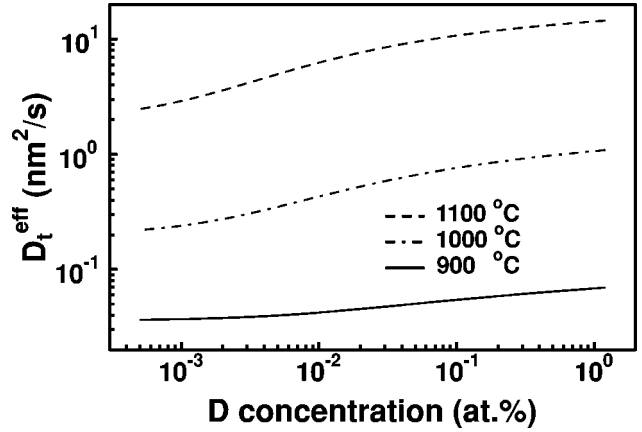


FIG. 1. Effective diffusion coefficient D_t^{eff} as a function of total D concentration at annealing temperatures 900, 1000, and 1100 °C.

IV. RESULTS AND DISCUSSION

The concentration profiles together with the numerical fits at annealing temperatures 900 °C for 1 h 40 min, and 1000 °C for 2 h, are shown in Fig. 2. The agreement between the experimental SIMS profiles and the theoretical fits is quite good, whereas the complementary error function also depicted in the figure does not reproduce the concentration distribution. The fittings were less successful in giving an accurate shape to the near-surface side of the profile. As can be seen in Fig. 2, after annealing at 1000 °C for 2 h the solubility limit on the deep side of the profile starts almost from the as-implanted profile, indicating that on this side the implantation-induced defects are negligible. On the near-surface side, the solubility limit starts from the depth 200 nm, i.e., about 50 nm from the as-implanted profile at the same concentration. This can be explained by the implantation induced defects which were simulated by SRIM-96 (Ref. 9), and also depicted in Fig. 2. The deposited energy curve shows that the implanted D loses most of its energy in the 200–350-nm region, producing material damage and en-

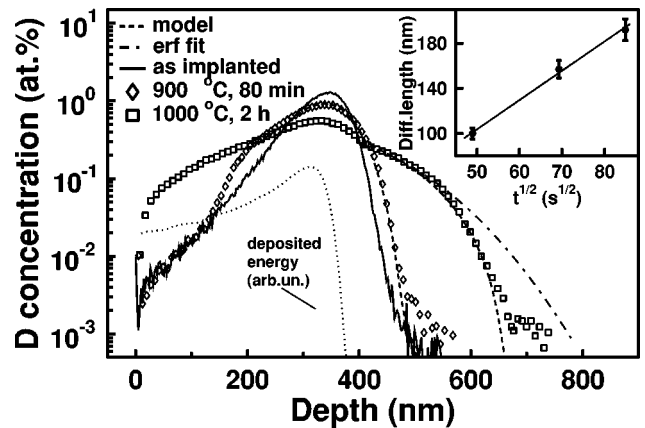


FIG. 2. Experimental deuterium depth profiles obtained after implantation and after annealing at different temperatures with numerical fits by the diffusion model (dashed line) and error function (dot-dashed line). The dotted line is the deposited energy calculated by SRIM-96. The inset shows D diffusion length vs square root of the annealing time for 1000 °C 40-, 80-, and 120-min annealings. The solid line is the linear fit to the experimental data.

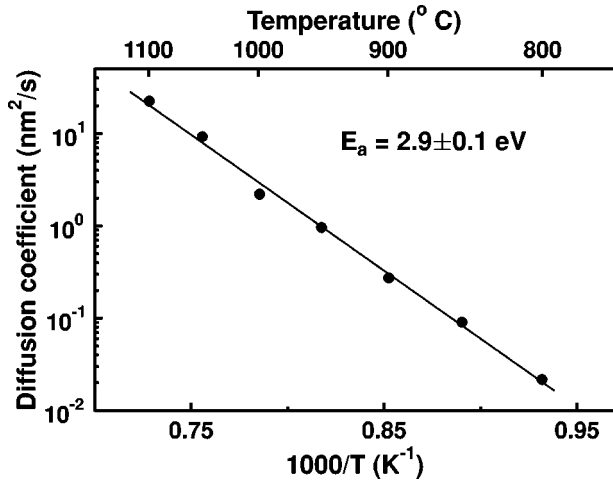


FIG. 3. Arrhenius plot for diffusion coefficient of atomic D. Shown are the natural logarithms of the diffusion coefficients vs $1000/T$. The solid line is the fit to the experimental data.

hanced D diffusion in this region. In the inset of Fig. 2, the diffusion length in the case of annealing at 1000 °C for 40, 80, and 120 min is plotted vs the square root of the annealing time. The diffusion length is defined here as the depth interval from the beginning of the concentration-dependent diffusion profile, i.e., at about 420 nm, where the solubility limit starts, to the end of the profile where the D concentration has decreased to the background level of about 3×10^{-3} at. %. The observed proportionality of the diffusion length to the square root of the annealing time is an indication of steady-state diffusion in homogeneous material. From the above, it follows that to obtain accurate diffusion parameters, fittings must be done only on deep side of the profile.

Figure 3 shows the Arrhenius plot for the D diffusion coefficient. The D diffusion is well described by the Arrhenius equation $D = D_0 \exp(-E_a/k_b T)$, where $D_0 = 1.1 \times 10^{12}$ nm²/s is the pre-exponential factor, and $E_a = 2.9 \pm 0.1$ eV the activation energy, k_b is Boltzmann's constant, and T is the absolute annealing temperature. In our previous paper, where diffusion of H in DLC was studied,⁵ no concentration-dependent diffusion was observed due to the initial hydrogen background of about 0.07 at. % in these films, whereas in the case of D the fits were made to the low concentration regime. This explains the difference in activation energies ($E_a = 2.0 \pm 0.1$ eV for H). Therefore, the diffusion coefficients for hydrogen and deuterium cannot be compared directly with each other. However, by employing the matrix method⁵ to fit D profiles, and choosing the lowest concentration limit of 0.07 at. %, one obtains an activation energy of 2.0 ± 0.1 eV, matching the value for H. The ratio of the pre-exponential factor for H to D in this case is 1.3, which comes from the isotope effect.

The fitting parameters, pairing constant K , and pairing exponents B and F defined in Eq. (6), are presented in Fig. 4. These parameters can be fairly well described by the equation

$$P = P_0 \exp(E/k_b T), \quad (9)$$

where P stands for the parameters K , B , or F , and P_0 for the pre-exponential factor for the corresponding parameter, and

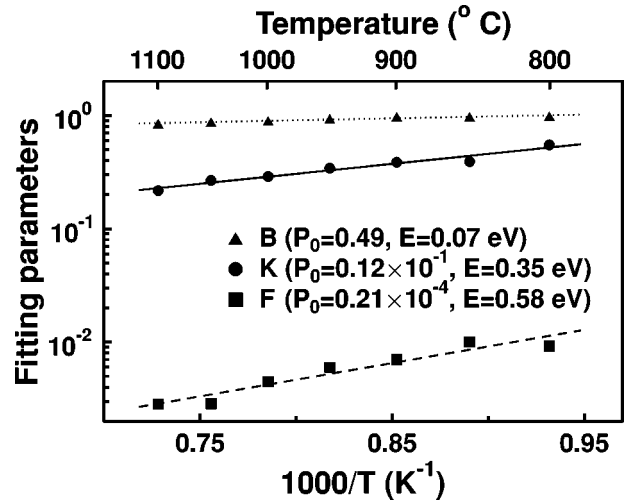


FIG. 4. Fitting parameters pairing constant K , and pairing exponents B and F with corresponding fits.

constant E has the meaning of activation energy. Both activation energies and pre-exponential factors are given in the figure. The exponential decrease of K with increasing temperature can be qualitatively explained by the increase of thermal energy to break the bonds between D pairs. The effect of the pairing exponent B can be seen in Fig. 5, where the atomic and paired concentrations at annealing temperature 1050 °C for 30 min are plotted as a function of depth. At lower concentrations, proportionally more immobile D pairs are formed, decreasing the effective diffusivity as seen in Fig. 1. The F parameter [see Eq. (6)] is needed to keep the concentration of D pairs smaller than the total D concentration, and to keep the effective diffusion coefficient [see Eq. (8)] positive. An explanation for this parameter might be the initial presence of hydrogen in these films,⁵ which can form H-H pairs, but, due to the much larger D concentration, most probably it will pair with D, forming immobile H-D complexes. This hydrogen was not directly measured, so we can speculate that parameter F is linked somehow to the hydrogen concentration. The decrease of parameter F , with increasing temperature, can be understood by the decrease of D solubility with temperature increase, which can be observed

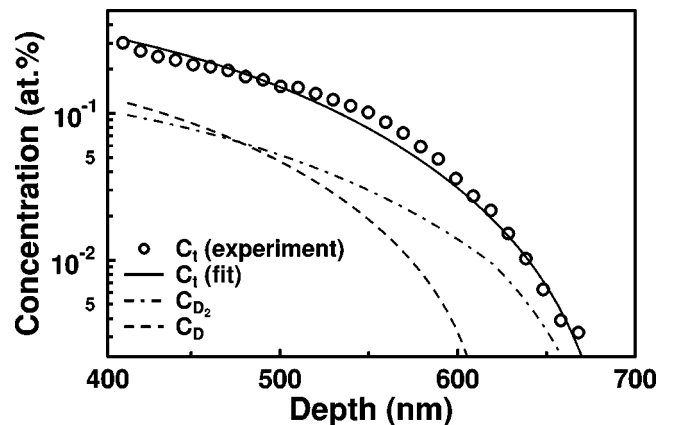


FIG. 5. Total deuterium concentration (the solid line is the fit to experimental results) at an annealing temperature 1050 °C for 30 min. Concentrations of atomic D and deuterium pairs are presented by dashed and dot-dashed lines, respectively.

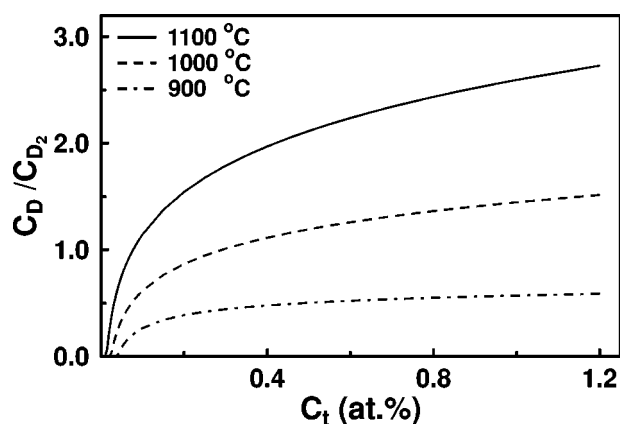


FIG. 6. Ratio of atomic deuterium to D pairs as a function of total concentration at different annealing temperatures.

from Fig. 2. On the other hand, the number of pairs decreases as a function of annealing temperature as explained above. The solid solubilities are 0.32 at. % at 1000 °C, 0.31 at. % at 1050 °C, and 0.26 at. % at the highest temperature 1100 °C.

The ratio of D atoms to the D pairs, theoretically calculated from Eqs. (6) and (7), as a function of total D concentration, is plotted for temperatures 900, 1000, and 1100 °C in Fig. 6. It may be noted that at high temperature and concentration the atomic D concentration is larger than the concentration of D pairs, while at lower temperatures a smaller

fraction of D can move leading to a high activation energy of 2.9 ± 0.1 eV compared to the value of 1.9 eV from Ref. 8. This value is an activation barrier for diffusion of atomic hydrogen from the BC site to a similar neighboring one, without taking into account the presence of the second H atom at the AB site. It should be stressed as well that diamond and DLC are different allotropic forms of carbon, and diffusivity of hydrogen isotopes in these materials can be different.

V. CONCLUSIONS

Migration of deuterium in D^+ -ion-implanted DLC film has been studied, and the obtained D depth profiles have been fitted with a concentration-dependent diffusion model, assuming that D exists as immobile pairs and diffusing atoms. The diffusion coefficient exhibits a good Arrhenius behavior with an activation energy of 2.9 ± 0.1 eV. A decreasing solid solubility of D in DLC films with increasing temperature was observed.

ACKNOWLEDGMENTS

This work was supported by the Association Euratom-TEKES within the Finnish fusion program (FFUSION). Jukka Kolehmainen and Janne Partanen (DIARC-Technology Inc.) are gratefully acknowledged for the sample preparation. Dr. Joseph Campbell (Helsinki University of Technology) is greatly acknowledged for comments on the manuscript.

*Corresponding author. Fax: +358 9 1918378; Electronic address: tahlgren@beam.helsinki.fi

†Permanent address: Technical Research Center of Finland, Chemical Technology, P.O. Box 1404, FIN-02044 VTT, Finland.

¹S. M. Sze, *Physics of Semiconductor Devices* (Wiley, New York, 1981), pp. 790–838.

²S. A. Kajihara, A. Antonelli, J. Bernholc, and R. Car, *Phys. Rev. Lett.* **66**, 2010 (1991).

³M. I. Landstrass and K. V. Ravi, *Appl. Phys. Lett.* **55**, 1391 (1989).

⁴M. I. Landstrass and K. V. Ravi, *Appl. Phys. Lett.* **55**, 975 (1989).

⁵E. Vainonen, J. Likonen, T. Ahlgren, P. Haussalo, J. Keinonen, and C. H. Wu, *J. Appl. Phys.* **82**, 3791 (1997).

⁶K. J. Chang and D. J. Chadi, *Phys. Rev. Lett.* **62**, 937 (1989).

⁷D. Mathiot, *Phys. Rev. B* **40**, 5867 (1989).

⁸S. P. Mehandru, A. P. Anderson, and J. C. Angus, *J. Mater. Res.* **7**, 689 (1992).

⁹J. F. Ziegler and J. P. Biersack, SRIM-96 computer code (private communication).